Published in final edited form as:
J Phys Chem B. 2010 June 17; 114(23): 7719–7726. doi:10.1021/jp9122216.

Structure and Self-Assembly Properties of a New Chitosan-Based Amphiphile

Yuping Huang[†], **Hailong Yu**[†], **Liang Guo**[‡], and **Qingrong Huang**[*,†]
Department of Food Science, Rutgers University, 65 Dudley Road, New Brunswick, New Jersey 08901, and BioCAT at APS/Argonne National Laboratory, Illinois Institute of Technology, Argonne, Illinois 60439

Abstract

A new chitosan-based amphiphile, octanoyl-chitosan-polyethylene glycol monomethyl ether (acylChitoMPEG), has been prepared using both hydrophobic octanoyl and hydrophilic polyethylene glycol monomethyl ether (MPEG) substitutions. The success of synthesis was confirmed by Fourier transform infrared (FT-IR) and ^{1}H NMR spectroscopy. The synthesized acylChitoMPEG exhibited good solubility in either aqueous solution or common organic solvents such as ethanol, acetone, and $CHCl_3$. The self-aggregation behavior of acylChitoMPEG in solutions was studied by a combination of pyrene fluorescence technique, dynamic light scattering, atomic force microscopy, and small-angle X-ray scattering (SAXS). The critical aggregation concentration (CAC) and hydrodynamic diameter were found to be 0.066 mg/mL and 24.4 nm, respectively. SAXS results suggested a coiled structure of the triple helical acylChitoMPEG backbone with the hydrophobic moieties hiding in the center of the backbone, and the hydrophilic MPEG chains surrounding the acylChitoMPEG backbone in a random Gaussian chain conformation. Cytotoxicity results showed that acylChitoMPEG exhibited negligible cytotoxicity even at concentrations as high as 1.0 mg/mL. All results implied that acylChitoMPEG has the potential to be used for biological or medical applications.

Introduction

Chitosan, mainly composed of two subunits, D-glucosamine (GlcN) and *N*-acetyl *β*-D-glucosamine linked by β (1→4) glycosidic bonds, is a fully or partially *N*-deacetylated product of naturally abundant chitin extracted from the shells of crabs, shrimp, and krill. It is known that chitosan exhibits several attractive characteristics such as biocompatibility, biodegradability, low-toxicity, and remarkable affinity to proteins, which help attract increasing attention in the fields of food, textile, cosmetics, biomedical, pharmaceutical, and other industries.[1–7] In particular, chitosan has been reported to be used as a material for drug delivery,[8,9] film-coating,[10] and tissue engineering applications.[11] More details may be found in the listed reviews and the references therein.[7,12,13]

[*]Author to whom correspondence should be addressed. Tel: 732-932-7193. Fax: 732-932-6776. qhuang@aesop.rutgers.edu.
[†]Rutgers University.
[‡]Argonne National Laboratory.

Supporting Information Available: Additional synthesis details; ^{1}H NMR full and partial enlarged spectra of chitosan, acylChitosan, and acylChitoMPEG; and solubility test of chitosan, acylChitosan, and acylChitoMPEG in water, anhydrous ethanol, acetone, methylene chloride, chloroform, tetrahydrofuran, and dioxide. This material is available free of charge via the Internet at http://pubs.acs.org.

Despite its apparent advantages, the poor solubility of chitosan in either water or common organic solvents due to its rigid crystalline structure has so far limited it from widespread utilization.[5] To overcome this drawback, it is necessary to convert chitosan to either water- or organic solvent-soluble derivatives for further biomedical applications. To develop biomaterials with advanced functionalities, many attempts have been made to modify the molecular structure of chitosan by introducing either a hydrophobic or a hydrophilic moiety into chitosan,[14] such as an alkyl group,[1,15] a tetradecenoyl group,[16] poly(ε-caprolactone),[17] cholesterol,[18] deoxycholic acid,[19–21] phthalic anhydride and triphenylchloromethane,[22] acetyl,[2] acrylic acid,[3] carboxymethyl, dihydroxyethyl, sulfuryl, phosphoryl groups, carbohydrate,[7] poly(ethylene glycol) (PEG),[4,23–29] and so forth, and thereby to improve or control the physical properties of chitosan. Among them, Sashiwa et al. carried out hydrophobic modification of chitosan using a series of acyl chlorides with an ester linkage to increase the solubility of chitosan derivatives in organic solvents,[15] and the ester linkage can be hydrolyzed by enzymes such as lipases. PEGylation of chitosan to increase its water solubility has also been extensively investigated by several authors because of PEG's outstanding physicochemical and biological properties, such as hydrophilicity, low-toxicity, ease of chemical modification and absence of antigenicity and immunogenicity. Moreover, it was reported that the PEGylation of chitosan derivatives could increase cell viability.[25]

Up to now there have been scarce experimental investigations on chitosan with both hydrophobic and hydrophilic modifications. Polymers composed of both hydrophobic and hydrophilic segments usually form micellar structures or micelle-like self-assemblies with hydrophobic inner cores and hydrophilic outer shells in aqueous media via intra- and/or intermolecular association of hydrophobic segments.[18,23,24] Such types of polymeric micelles have been employed as delivery vehicles for bioactive agents of poor solubility.[24]

In this paper we describe the synthesis of a new biomaterial on the basis of chitosan modified with acyl chloride for the hydrophobic group and polyethylene glycol monomethyl ether (MPEG) for the hydrophilic group (abbreviated as acylChitoMPEG). The modified chitosan was characterized with Fourier transform infrared (FT-IR), fluorescence, and ^{1}H NMR spectroscopy. The solubility and thermal properties of acylChitoMPEG were examined. The self-assembly behavior of acylChitoMPEG in aqueous solutions was studied with pyrene fluorescence, dynamic light scattering (DLS), and small-angle X-ray scattering (SAXS). The morphology of the acylChitoMPEG nanoparticles was probed by atomic force microscopy (AFM). The cytotoxicity of acylChitoMPEG was evaluated for its applicability as a drug/gene delivery vehicle.

Experimental Section

Materials

Chitosan [molecular weight (MW) = 10 000 g/mol, deacetylation degree = 74.0%] was purchased from Kitto Life Co., Ltd. (South Korea). Octanoyl chloride, methane-sulfonic acid ($MeSO_3H$), MPEG (MW = 2000 g/mol), succinic anhydride, dichloromethane (CH_2Cl_2, extra dry), *N*-hydroxysuccinimide (NHS), *N*,*N*′-dicyclohexyl carbodiimide (DCC), dimethyl sulfoxide (DMSO, anhydrous), deuteriochloroform ($CDCl_3$), and deuterium oxide (D_2O) were obtained from Sigma-Aldrich Co. Ltd., USA, and used as received. Sodium bicarbonate ($NaHCO_3$) and ethyl ether were purchased from Fisher Co. Ltd., USA. Pyrene was obtained from Alfa Aesar, Co., USA. Dialysis tubings (MW cutoff = 1000 or 6000–8000 g/mol) were purchased from Spectrum Medical Industries, Inc., USA. Human hepatocellular caricinoma cells (HepG2) were obtained from American Type Culture Collection (HB-8065), and cultured in minimum essential medium (Invitrogen) containing 10% fetal bovine serum (Invitrogen), 100 units/mL penicillin (Invitrogen), and 100 μg/mL

streptomycin (Invitrogen). Cells were maintained at 37 °C with 95% relative humidity and 5% CO_2.

Preparation of AcylChitoMPEG

AcylChitoMPEG was prepared from chitosan through several processes, including acylation, esterification, etc. The preparation route for acylChitoMPEG is shown in Scheme 1. Further details on the synthesis can be found in Supporting Information. The structures of chitosan and its derivatives were characterized by FT-IR and ^{1}H NMR.

Attenuated Total Reflectance Fourier Transform Infrared (ATR-FTIR) Spectroscopy

The ATR-FTIR spectra were collected under ambient conditions, using a Thermal Nicolet Nexus 670 FT-IR spectrometer (Thermo Electron Corp., Madison, WI) with a Smart MIRacle horizontal attenuated total reflectance Ge crystal accessory. Each spectrum was averaged over 256 scans with 4 cm^{-1} resolution.

Measurement of Thermal Transitions

Differential scanning calorimetry (DSC) (DSC823^e, Mettler Toledo) was used to determine the thermal properties of MPEG, chitosan, and acylChitoMPEG. Samples of approximatly 5 mg were first heated from 20 to 200 °C with a heating rate of 20 °C/min. They were then quenched to 0 °C at a cooling rate of −20 °C/min with liquid nitrogen, followed by a second heating run at the same rate of 20 °C/min under air atmosphere.[30,31] The glass transition temperature (T_g) was taken by calculating the temperature of the half step height during the second heating run, while the melting temperature (T_m) was determined from the endothermic peak of the DSC curve recorded in the second heating scan.

Solubility Test

The solubility of chitosan and its derivatives in water and several organic solvents was evaluated by visual observation. The samples were soaked in each solvent at a concentration of 5 mg/mL at room temperature, and the solubility after 24 h was examined.

Measurement of Critical Aggregation Concentration (CAC) of acylChitoMPEG

The CAC of acylChitoMPEG in aqueous media was monitored by fluorescence spectroscopy with pyrene as the fluorescence probe. A pyrene stock solution (1.0×10^{-3} M) in methanol was added into the test tubes, and the methanol was removed under a stream of nitrogen gas. Then, acylChitoMPEG solutions in Milli-Q water of different concentrations were added into the above test tubes, making the final concentration of pyrene 1.0×10^{-6} M, which was nearly equal to the solubility of pyrene in water at 22 °C.[5,32] The mixtures were sonicated for 30 min in an ultrasonic bath at room temperature. Pyrene emission spectra were obtained using a fluorescence spectrophotometer (Cary Eclipse, Varian). The probe was excited at 343 nm, and the emission spectra were recorded in the range of 350–500 nm. The excitation and emission slit widths were 10 and 2.5 nm, respectively.

Atomic Force Microscopy

Morphological evaluation of acylChitoMPEG nanoparticles was performed with AFM. Sample solutions were dripped on a freshly cleaved mica surface, predried in the air for 1 h, and then dried under a stream of nitrogen gas. All AFM images were recorded in tapping mode using a Nanoscope IIIA Multimode AFM (Veeco Metrology, Santa Barbara, CA) at room temperature. A silicon tip with nominal spring constant of 40 N/m was used.

Dynamic Light Scattering

The mean hydrodynamic diameter of acylChitoMPEG nanoparticles was determined using a DLS-based BIC 90 plus particle size analyzer equipped with a Brookhaven BI-9000AT digital correlator (Brookhaven Instrument Corporation, New York) at a fixed scattering angle of 90° at room temperature. The light source of the particle size analyzer is a solid state laser operating at 658 nm with 30 mW power, and the signals were detected by a high sensitivity avalanche photodiode detector. The normalized field–field autocorrelation function $g(q,t)$ is obtained from the intensity–intensity autocorrelation function, $G(q,t)$, via the Sigert relation:

$$\alpha g(q,t)=[G(q,t)/A-1]^{1/2} \quad (1)$$

where A is the experimentally determined baseline, α is the contrast factor, which is less than 1, due to the fact that only a fraction of dynamic scattering intensity falls within the correlator window and also the fact that a finite size pinhole is used in the experiment. For each particle size measurement, the measured baseline A is in agreement with the theoretically calculated baseline to 0.01%.

The William–Watts (WW) single stretched exponential function was utilized in the fitting of the autocorrelation function:

$$g(q,t)=\exp[-(t/\tau)^{\beta}] \quad (2)$$

Here β is a parameter that describes the polydispersity of diffusing particles. For monodisperse nanoparticles, $\beta = 1$ is expected; for a polydisperse system, $0 < \beta < 1$.

The diffusion coefficient D was calculated according to $D = \tau^{-1}q^{-2}$, where q is the amplitude of scattering vector defined as $q = (4\pi n/\lambda)\sin(\theta/2)$, n is the solution refractive index, λ is the laser wavelength, and θ is the scattering angle. The diffusion coefficient D can be converted into mean nanoparticle diameter d using the Stokes–Einstein equation:

$$d=\frac{kT}{2\pi\eta D} \quad (3)$$

where k is the Boltzmann constant, T is the absolute temperature, and η is the solvent viscosity.

Small-Angle X-ray Scattering

SAXS data were acquired at the BioCAT, 18-ID beamline, at the Advanced Photon Source, Argonne National Laboratory. Two experimental setups of a sample–detector distance of 2.592 and 0.851 m were used to cover a combined Q range of 0.006–0.9 $Å^{-1}$ (with an Mar165 CCD being offset laterally relative to the X-ray beam). A flow cell of 1.5 mm diameter quartz capillary fitted to a brass block (thermostatted with a water bath) was used for holding samples, and the whole sample holder was maintained at 25 °C in the experiments. A MICROLAB 500 Hamilton pump was used to load samples to the flow cell, and to flow the samples at a constant rate (10 μL/s) during X-ray exposure for minimizing radiation damage. The X-ray wavelength was 1.033 Å, and the full beam flux used for measurements was 10^{13} photons/s for the longer camera length but attenuated for the shorter camera length to prevent detector saturation by signals from high concentration solutions. A single exposure of 1 s was used to acquire the scattering data, and identical measurement

configurations were used for the solvent background and the sample solutions for proper background subtraction. The scattering data at the two camera lengths were merged to produce a single scattering profile, and were shown on absolute scale by calibrating with the scattering of water.[33]

Cytotoxicity Test

Cell cytotoxicity was evaluated by 3-[4,5-dimethyl-thiazol-2-yl]-2,5-diphenyl tetrazolium bromide (MTT) assay as described previously,[34] but with some modifications. Briefly, HepG2 cells were plated in 96-well plates at a density of 10 000 cells per well in a final volume of 100 μL medium. After 24 h, the cells were treated with acylChitoMPEG at different concentrations for another 24 h. And then cell culture medium was aspirated and cells were incubated with 100 μL of MTT solution (0.5 mg/mL in RPMI 1640 medium) for 2 h at 37 °C. Subsequently, the MTT solution was carefully aspirated, and the formazan crystals formed were dissolved in 100 μL DMSO per well. Light absorbance at 560 and 670 nm was recorded with an Absorbance Microplate Reader (Molecular Devices). Relative cell viability was expressed as A560-A670 normalized to that of the untreated wells. Data were presented as mean ± standard deviation with eight well repeats.

Results and Discussion

Characterization

Figure 1 shows the FT-IR spectra of chitosan and its derivatives. In comparison with chitosan, the FT-IR spectrum of acylChitoMPEG presented new absorption peaks at ~1740 cm^{-1}, which were assigned to octanoyl groups, as well as ~840, 950, and 2880 cm^{-1} peaks, which arose from the MPEG segment. Meanwhile, a decrease was observed in the relative intensity of the broad peak at 3200–3500 cm^{-1} corresponding to the hydroxyl and amino groups within chitosan. These results suggested that octanoyl groups and MPEG were grafted to the backbone of chitosan.

Additional information of the chitosan and its derivatives was obtained by ^{1}H NMR analysis (see Supporting Information). The peaks specific to chitosan appeared between 1.8 and 5.2 ppm. The new peaks at 0.88, 1.28, 1.61, and 2.34 ppm, which originated from the ^{1}H NMR spectrum of acylChitosan, were mainly due to the characteristic alkyl protons of the reacted chitosan with acyl chloride. These peaks showed the presence of major functional groups linked to chitosan. The degree of substitution (DS) was calculated following the method of Sashiwa et al.[1,2,15] The DS of the R group, DS(NHR + OR), was estimated by comparing the ratio of methyl protons (δ 0.88, Me, 3z H) to sugar protons [δ 2.7–5.2, (9–*z*) H]. DS(NH-$COCH_3$, 3*y*) was obtained from δ 1.9–2.1 versus δ 3.2–5.2. DS(NH_2, *x*) was estimated from δ 2.7–2.8 (*x*) versus δ 3.2–5.2. DS(NHR) = $1 - x - y$ and DS(OR) = DS(NHR + OR) − DS(NHR). The above DS values are shown in Table 1.

Compared to the spectrum of chitosan, peaks corresponding to the $–COCH_2CH_2CO–$group of the acylChitoMPEG molecule appeared at 2.6–2.7 ppm on its ^{1}H NMR spectrum, and the sharp single-peak signal at 3.4 ppm was assigned to the $–OCH_3$ of MPEG segments. The ratio between the DS of acyl groups (DS_R) and that of MPEG (DS_M), was estimated by the proton integration ratio between δ 0.88 (CH_3) and δ 3.4 ($–OCH_3$) in ^{1}H NMR spectrum, and its value was about 2.18 (see Table 2). Because the peaks of H-2, 3, 4, 5, 6, and OH of chitosan except for H-2 of GlcN were overlapped with those of the $(–OCH_2CH_2–)_m$ group in MPEG segments, it was difficult to evaluate the DS of MPEG (DS_M) directly. In the process of preparing acylChitoMPEG, the DS of acyl groups (DS_R) could not be changed and was still equal to DS(NHR + OR), so DS_M could be calculated by DS(NHR + OR) and (DS_R/DS_M), and its value was about 0.46. According to the DS of the functional groups, the

molecular formula of repeating units of acylChitoMPEG could be written as $C_6H_7O_2(OH)_{1.08}(OR)_{0.92}(NH_2)_{0.23}$-$(NHCOCH_3)_{0.23}(NHR)_{0.08}(NHCOCH_2CH_2COMPEG)_{0.46}$. Consequently, the MW of acylChitoMPEG was calculated as 72.8k from the ^{1}H NMR data.

Thermal Properties

The glass transition temperature (T_g) of a material affects its mechanical property. Dong et al. considered 140–150 °C as the T_g of chitosan by means of four techniques.[35] To eliminate the effects of moisture and thermal history, two cycles of heating and cooling runs were adopted. The first heating run of initial chitosan gave a single endothermic peak at about 100 °C, attributed to absorbed moisture.

Figure 2 showed the DSC curves of chitosan (Figure 2 inset), MPEG, and acylChitoMPEG obtained from the second heating run. The T_g of chitosan observed was 146.1 °C, which is consistent with the result reported by Dong et al. The melting behaviors of MPEG and acylChitoMPEG were also investigated in the second heating scan. DSC thermograms showed an endothermic peak at its melting temperature for MPEG. T_m of MPEG was 53.9 °C, and the endothermic peak of acylChitoMPEG appeared at 51.9 °C, corresponding to the melting transition of the MPEG segment, with a decrease of 2 °C, which implied that the crystallization of MPEG was slightly affected by the chitosan backbone. However, there was no obvious baseline step on the second heating curve for acylChitoMPEG in the measured temperature range, implying that the glass transition of chitosan was nearly suppressed by MPEG segments.

Solubility Test

Solubility test was carried out according to the method reported by Feng et al.[6] and Hu et al.[26] The results of the solubility tests (pictures can be found in the Supporting Information) at room temperature are summarized in Table 3. In comparison with the original chitosan, acylChitosan exhibited good solubility in some common organic solvents, but it became water-insoluble because of the introduction of hydrophobic octanoyl groups. When the hydrophilic MPEG chains were further introduced on the amino groups of acylChitosan, the product acylChitoMPEG became water-soluble again. It was also soluble in organic solvents, exhibiting amphiphilic properties. This result indicated that the attachment of octanoyl groups and MPEG chains modified the hydrophobicity–hydrophilicity balance of the acylChitoMPEG, as well as the intra- and/or intermolecular hydrogen bonding of chitosan backbone. The improved solubility makes acylChitoMPEG more versatile in being fabricated into various micro- and/or nanoparticles, extending the application range of chitosan derivatives in the biomedical field.

Self-Assembly Properties

The CAC for the self-assembly of acylChitoMPEG was first examined with the pyrene fluorescence technique, a common method for measuring the CAC of polymeric amphiphiles. Pyrene is a poorly soluble and self-quenching agent in a polar environment, but strongly emits radiation when self-aggregates or other hydrophobic micro-domains are formed in an aqueous solution, as it prefers to be close to (or inside) the microdomain.[18] There are five vibronic peaks in the pyrene emission spectra. Figure 3a showed the typical emission spectrum of pyrene in acylChitoMPEG solution. The intensity ratio of the first peak and the third peak, I_1/I_3, is quite sensitive to the polarity of the microenvironment and has been frequently used as an indicator for a subtle change of its environment. Hence, the CAC, which is defined as the incept concentration of self-aggregate formation by intra- and/or intermolecular association, can be determined from the change of the I_1/I_3 value of pyrene in the presence of polymeric amphiphiles.[36,37] Figure 3b illustrated the changes of

the I_1/I_3 values as a function of acylChitoMPEG concentrations. At low concentrations, the I_1/I_3 values were close to the value (1.84) of pyrene in water,[38] and then followed by a linear decrease with further increase of concentration, implying the onset of self-association of acylChitoMPEG. The CAC of acylChitoMPEG could be determined as the intercept of two straight lines, and its value was 6.6×10^{-2} mg/mL (see Table 4). However, for chitosan solution, it was previously reported by Amiji that a significant decrease of the I_1/I_3 value was observed only at chitosan concentrations above 1.0 mg/mL.[39] It could be deduced that the aggregation of acylChitoMPEG molecules in aqueous media may be mainly due to the hydrophobic interactions of alkyl chains.

The morphology of the acylChitoMPEG nanoparticles was further observed by tapping-mode AFM, as depicted in Figure 4a. The nanoparticles were sphere-like. By averaging the vertical distances of nanoparticles in the height mode using the section analysis, we can obtain the mean apparent particle diameter of 17.6 nm. The mean hydrodynamic diameter of acylChitoMPEG nanoparticles was also measured by means of the DLS method at room temperature. Figure 4b showed the DLS autocorrelation function curve of acylChitoMPEG dissolved in Milli-Q water, as well as its fitting curve analyzed by a single stretched exponential fit. The values of the mean apparent particle diameter and hydrodynamic diameter are listed in Table 4. The particle size from AFM was slightly smaller than that from DLS, which was mainly due to the process involved in the preparation of the samples. It was known that the AFM gave the images of the particles in the dry state, while DLS depicted the value of the particle size in solution of the sample. The size determined by DLS included hydrated layers surrounding the nanoparticles, and was therefore larger than that in dry state determined by AFM.

Structure Analysis

The structure of acylChitoMPEG had been also studied by SAXS. Figure 5 showed the scattering profile of the acylChitoMPEG sample in water at concentrations of 1.3, 2.5, 5, 10, and 20 mg/mL, respectively (solid symbols). Except at the highest concentration of 20 mg/mL, the scattering profile of all other concentrations indicated limited particle size and a globular particle shape. The globular particle shape was also indicated by the bell shape of the pair-distribution function, calculated with the program GNOM,[40] and shown as lines in the inset for concentrations of 2.5, 5, and 10 mg/mL using data up to $Q = 0.5$ Å^{-1}. The pair-distribution profiles also indicated that the maximum dimension of the nanoparticle was around 180 Å.

For micelles or aggregates of limited particle sizes, the association number n, i.e., the number of molecules in one particle, can be calculated through the forward scattering:

$$I(Q=0)=c \times n \times \Delta b^2/M \quad (4)$$

where I is the scattering intensity, c is the sample concentration, Δb is the scattering length difference of one molecule relative to the surrounding medium, and M is the molecular weight of the molecule.

The scattering length difference Δb of one acylChitoMPEG molecule relative to water was 0.0874 Å (assuming chitosan density 1.4 g/cm^3, octanoyl group density 0.91 g/cm^3, and MPEG density 1.1 g/cm^3). The forward scattering $I(Q = 0)$ was obtained through a Guinier fit of the scattering profile in the low Q range (the scattering intercept at $Q = 0$). The fitted forward scattering value and the calculated association number are listed in Table 5 for the acylChitoMPEG sample (MW = 72.8 kD) at the five measured concentrations. It was noted that the average association number was 3.3, which basically did not change with

concentration. This indicated that a change in concentration only led to a change in the number of particles (or micelles) formed without changing the number of molecules in individual particles. The basically unchanged particle size (R_g ~ 53 Å) at different concentrations and the similar scattering profile indicated that molecules assembled in the same way to form similar structures of the assembled nanoparticles at different concentrations. This was a desirable property in certain applications of controlled drug and/or gene delivery where the release property was not affected by the intake level of the carrier and its concentration within the human body.

The unmodified 10kD chitosan molecules are soluble in water at acidic or neutral pH, and the molecule backbone carries positive charges. Due to the repulsion of these positive charges, the backbone of chitosan molecule takes stretched, extended conformation, and in most cases a rod-like shape for unmodified native chitosan. The SAXS data of native chitosan solution in water shows a form factor close to a rod-like object. Hence, modified Guinier analysis for rod-like polymers was employed, as shown in Figure 6A, which involved plotting ln[Q•$I(Q)$] versus Q^2.[41] The cross-sectional radius of gyration of the rod R_c, which was calculated from the slope of the straight line ($R_c^2 = -2$ • slope) in the low Q region (Q_{max} • $R_c < 1$), is about 3.5 Å (or the rod diameter of ~7 Å), and is basically the dimension of an individual polysaccharide backbone. Grafting of both hydrophobic and hydrophilic chains to the chitosan molecule backbone at certain grafting ratio will change the rod shape, bending or twisting it into a coil or loop conformation. However, it is expected that a completely collapsed shape is not possible due to the repulsion of positive charges. In fact, the scattering profile of acylChitoMPEG can also be fitted by Pedersen's core-chain model,[42] which considered the structure of spherical micelles to consist of a spherical core with a radius of 4 Å surrounded by a shell of dissolved polymer chains with R_g of 26 Å (the solid line in Figure 5). The full stretched length of a 10 kD chitosan molecule is about 350 Å, which is approximately twice the maximum dimension (180 Å) of the acylChitoMPEG particle as obtained in the pair-distribution function (Figure 5 inset). This means that the acylChitoMPEG molecule was not fully stretched in a rod shape. On the other hand, since the acylChitoMPEG molecules cannot completely collapse to hide their hydrophobic moieties away from water molecules, it was expected that different acylChitoMPEG molecules will wrap around each other to shield their hydrophobic moieties from water. In the case of this study, three acylChitoMPEG molecules wrapped together, and a triple helical structure was expected since the wrapped backbone must bend or coil to accommodate a size limit of about 180 Å, as determined from the pair-distribution profile. We expected a coiled structure of the triple helical acylChitoMPEG backbone with the hydrophobic moieties hiding in the center of the backbone, and the hydrophilic MPEG chains surrounding the acylChitoMPEG backbone in a random Gaussian chain conformation (Scheme 2). A Gaussian chain conformation for the MPEG chain in water was also supported by our SAXS data shown in Figure 6B. By fitting the scattering profile of 2k MPEG to the Debye function for flexible, Gaussian polymer chains, which can be described as $I(q) = [2/(QR_g)^4][\exp(-Q^2R_g^2) + Q^2R_g^2 - 1]$, one found that the radius of gyration (R_g) of 2k MPEG was about 16 Å, implying a maximum dimension of 48 Å for a swollen Gaussian chain with excluded volume. This indicated that the acylChitoMPEG triple helical backbone bends into a dimension of ~80 Å, and the surrounding MPEG chains around the acylChitoMPEG back-bone extended the particle size to 180 Å. The broad peak at Q around 0.21 $Å^{-1}$ in the scattering profile of all concentrations indicated a characteristic interfering distance of 30 Å. We interpreted this distance as the distance between the polysaccharide backbones of the three chitosan molecules in the wrapped triple helix. This corresponded well to the stretched length of the grafted hydrophobic chains from the polysaccharide backbone to the grafted chain tip (13 Å).

The scattering profile at the highest concentration (20 mg/mL) had a power law slope of −2 in the low *Q* region, and this might indicate the formation of large scale agglomeration of associated particles in a structure of mass fractals of two dimensions or large disk-like objects.

Cytotoxicity Analysis

The synthesized polymer was amphiphilic in nature and has the potential to be used as drug/gene or food-ingredient delivery vehicles for biomedical and food applications. An ideal delivery platform must be biodegradable, biocompatible, and should not be associated with incidental adverse effects. The biocompatibility of the synthesized acylChitoMPEG was examined with MTT assay on HepG2 cells to determine its cytotoxicity. Figure 7 showed that no evidence of toxicity in cell viability assays was found in the concentration range from 0.1 μg/mL to 1.0 mg/mL of acylChitoMPEG. In the experiment, the half maximal inhibitory concentration (IC_{50}) of acylChitoMPEG was not detected even at a concentration as high as 1.0 mg/mL, where the cell viability was still as high as 100%. It might be that substitution with an alkyl group and MPEG moiety on the $–NH_2$ group of chitosan reduced the amount of polycations, and the primary amine groups on chitosan had a much lower chance to aggregate on the cell membrane surface to affect important cell function.[34,43] This suggested that the synthesized acylChitoMPEG is very biocompatible and can be used in biomedical areas and as encapsulation agents of active food ingredients.

Conclusion

In summary, a novel biopolymeric amphiphile, acylChitoMPEG was synthesized and characterized using various physicochemical spectral and thermal analysis methods. In addition, the solubility, CAC, particle size, particle morphology, structure of self-assemblies, and cytotoxicity of this amphiphile were systematically investigated. At current hydrophobic octanoyl and hydrophilic MPEG compositions, acylChitoMPEG behaved as a spherical shape in aqueous solutions with a hydrodynamic diameter of 24.4 nm. At acylChitoMPEG concentration below 20 mg/mL, a change in concentration only led to a change in the number of particles without changing the number of molecules in individual particles, which shows a desirable property in controlled drug and/or gene delivery where the release properties were not affected by the intake level of the carrier and its concentration within the human body. Due to its negligible cytotoxicity, acylChitoMPEG has the potential to be used in biological or medical fields. Further investigations are still in progress toward understanding of the effects of acyl chloride chain length and the ratio of chitosan to acyl chloride or MPEG on the size, structure, and morphology of the nanoparticles formed by acylChitoMPEG at different physicochemical conditions.

Supplementary Material

Refer to Web version on PubMed Central for supplementary material.

Acknowledgments

We thank Professor Jozef Kokini for the use of DSC. This work was supported by United States Department of Agriculture National Research Initiative (#2009-35603-05071). Use of the Advanced Photon Source was supported by the U.S. Department of Energy, Basic Energy Sciences, Office of Science, under contract No. W-31-109-ENG-38. BioCAT is a National Institutes of Health-supported Research Center RR-08630.

References and Notes

1. Sashiwa H, Kawasaki N, Nakayama A, Muraki E, Yamamoto N, Zhu H, Nagano H, Omura Y, Saimoto H, Shigemasa Y, Aiba S-i. Biomacromolecules. 2002; 3:1120. [PubMed: 12217062]

2. Sashiwa H, Kawasaki N, Nakayama A, Muraki E, Yamamoto N, Aiba S-i. Biomacromolecules. 2002; 3:1126. [PubMed: 12217063]
3. Sashiwa H, Yamamoto N, Ichinose Y, Sunamoto J, Aiba S-i. Macromol Biosci. 2003; 3:231.
4. Jeong YI, Kim DG, Jang MK, Nah JW. Carbohydr Res. 2008; 343:282. [PubMed: 18035341]
5. Liu KH, Chen SY, Liu DM, Liu TY. Macromolecules. 2008; 41:6511.
6. Feng H, Dong CM. Biomacromolecules. 2006; 7:3069. [PubMed: 17096533]
7. Rinaudo M. Prog Polym Sci. 2006; 31:603.
8. Tanuma H, Kiuchi H, Kai W, Yazawa K, Inoue Y. J Appl Polym Sci. 2009; 114:1902.
9. Shu S, Zhang X, Teng D, Wang Z, Li C. Carbohydr Res. 2009; 344:1197. [PubMed: 19508912]
10. Domján A, Bajdik J, Pintye-Hódi K. Macromolecules. 2009; 42:4667.
11. Hong H, Liu C, Wu W. J Appl Polym Sci. 2009; 114:1220.
12. Arvanitoyannis IS. J Macromol Sci - Rev Macromol Chem Phys. 1999; C39:205.
13. Kumar MNVR, Muzzarelli RAA, Muzzarelli C, Sashiwa H, Domb AJ. J Chem Rev. 2004; 104:6017.
14. Kurita K. Prog Polym Sci. 2001; 21:1921.
15. Sashiwa H, Kawasaki N, Nakayama A, Muraki E, Yamamoto N, Arvanitoyannis I, Zhu H, Aiba S-i. Chem Lett. 2002:598.
16. Zhang X, Ercelen S, Duportail G, Schaub E, Tikhonov V, Slita A, Zarubaev V, Babak V, Mely Y. J Gene Med. 2008; 10:527. [PubMed: 18265422]
17. Yu H, Wang W, Chen X, Deng C, Jing X. Biopolymers. 2006; 83:233. [PubMed: 16761262]
18. Wang YS, Liu LR, Jiang Q, Zhang QQ. Eur Polym J. 2007; 43:43.
19. Kim YH, Gihm SH, Park CR, Lee KY, Kim TW, Kwon IC, Chung H, Jeong SY. Bioconjugate Chem. 2001; 12:932.
20. Lee KY, Kwon IC, Kim YH, Jo WH, Jeong SY. J Controlled Release. 1998; 51:213.
21. Lee KY, Jo WH, Kwon IC, Kim YH, Jeong SY. Langmuir. 1998; 14:2329.
22. Nishimura SI, Kohgo O, Kurita K. Macromolecules. 1991; 24:4745.
23. Ouchi T, Nishizawa H, Ohya Y. Polymer. 1998; 39:5171.
24. Kim DG, Jeong YI, Nah JW. J Appl Polym Sci. 2007; 105:3246.
25. Mao S, Shuai X, Unger F, Wittmar M, Xie X, Kissel T. Biomaterials. 2005; 26:6343. [PubMed: 15913769]
26. Hu Y, Jiang H, Xu C, Wang Y, Zhu K. Carbohydr Polym. 2005; 61:472.
27. Saito H, Wu X, Harris JM, Hoffman AS. Macromol Rapid Commun. 1997; 18:547.
28. Kolhe P, Kannan RM. Biomaromolecules. 2003; 4:173.
29. Sashiwa H, Yamamori N, Ichinose Y, Sunamoto J, Aiba S-i. Biomacromolecules. 2003; 4:1250. [PubMed: 12959591]
30. Radhakumary C, Nair PD, Mathew S, Nair CPR. Trends Biomater Artif Organs. 2005; 18:117.
31. Picker-Freyer KM, Brink D. AAPS PharmSciTech. 2006; 7:E1. [PubMed: 16584139]
32. Wilhelm M, Zhao CL, Wang Y, Xu R, Winnik MA, Mura JL, Riess G, Croucher MD. Macromolecules. 1991; 24:1033.
33. Dreiss CA, Jack KS, Parker AP. J Appl Crystallogr. 2006; 39:32.
34. Wong K, Sun G, Zhang X, Dai H, Liu Y, He C, Leong KW. Bioconjugate Chem. 2006; 17:152.
35. Dong YM, Ruan YH, Wang HW, Zhao YG, Bi DX. J Appl Polym Sci. 2004; 93:1553.
36. Liu CG, Desai KGH, Chen XG, Park HJ. J Agric Food Chem. 2005; 53:437. [PubMed: 15656685]
37. Kalyanasundaram K, Thomas JK. J Am Chem Soc. 1977; 99:2039.
38. Dong DC, Winnik MA. Can J Chem. 1984; 62:2560.
39. Amiji MM. Carbohydr Polym. 1995; 26:211.
40. Svergun DI. J Appl Crystallogr. 1992; 25:495.
41. Porod, G. Small Angle X-Ray Scattering. Glatter, O.; Kratky, O., editors. Vol. Chapter 2. Academic Press; New York: 1982. p. 17-51.
42. Pedersen JS, Gerstenberg MC. Macromolecules. 1996; 29:1363.

43. Bottega R, Epand RM. Biochemistry. 1992; 31:9025. [PubMed: 1390689]

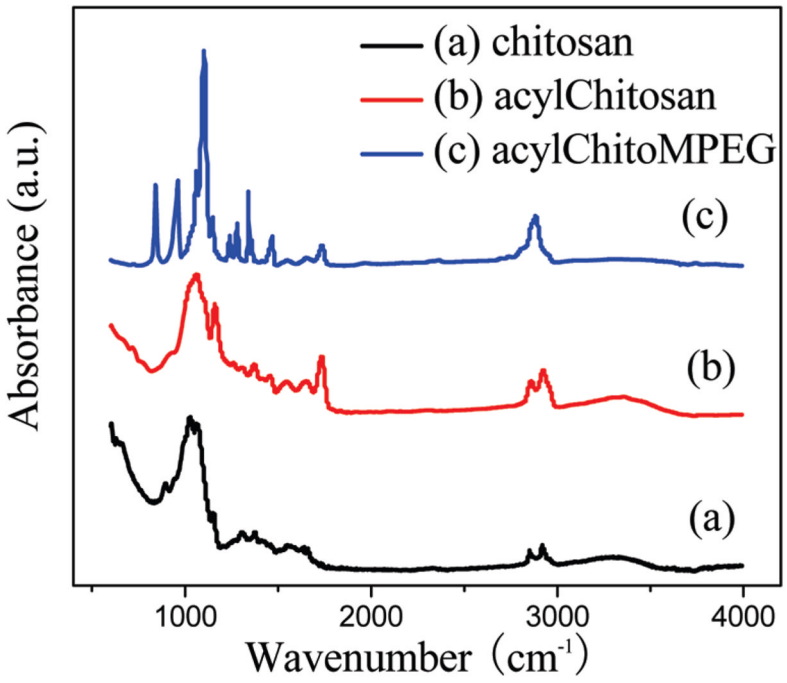

Figure 1.
FT-IR spectra of (a) chitosan, (b) acylChitosan, and (c) acylChitoMPEG.

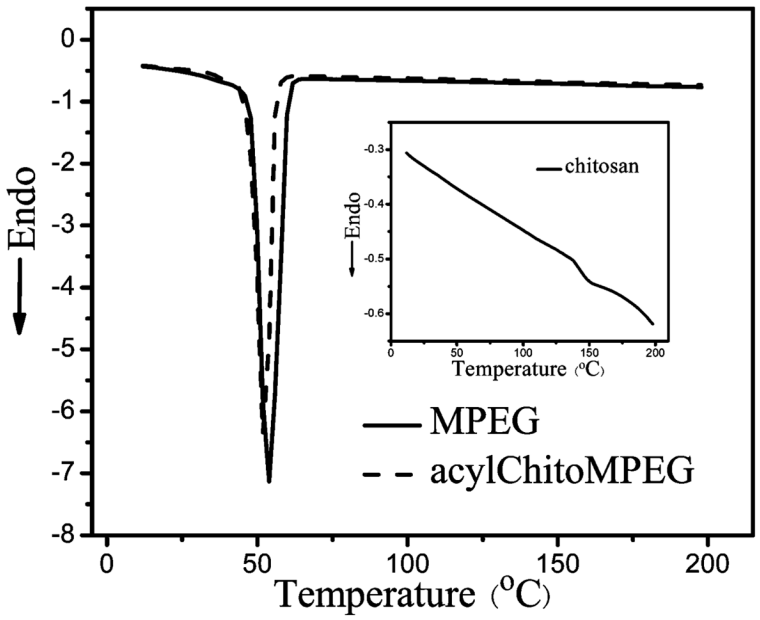

Figure 2.
DSC curve of MPEG and acylChitoMPEG obtained from the second heating run, and the inset showed the DSC curve of chitosan.

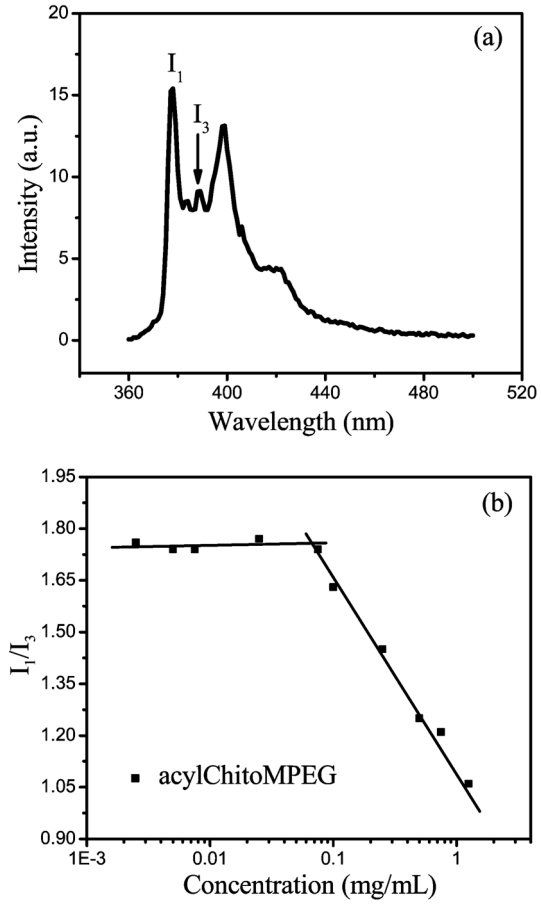

Figure 3.
(a) Emission spectra of pyrene in acylChitoMPEG solution with a concentration of 0.001 mg/mL. (b) Change of the intensity ratio (I_1/I_3) from excitation spectra of pyrene with various concentrations of acylChitoMPEG.

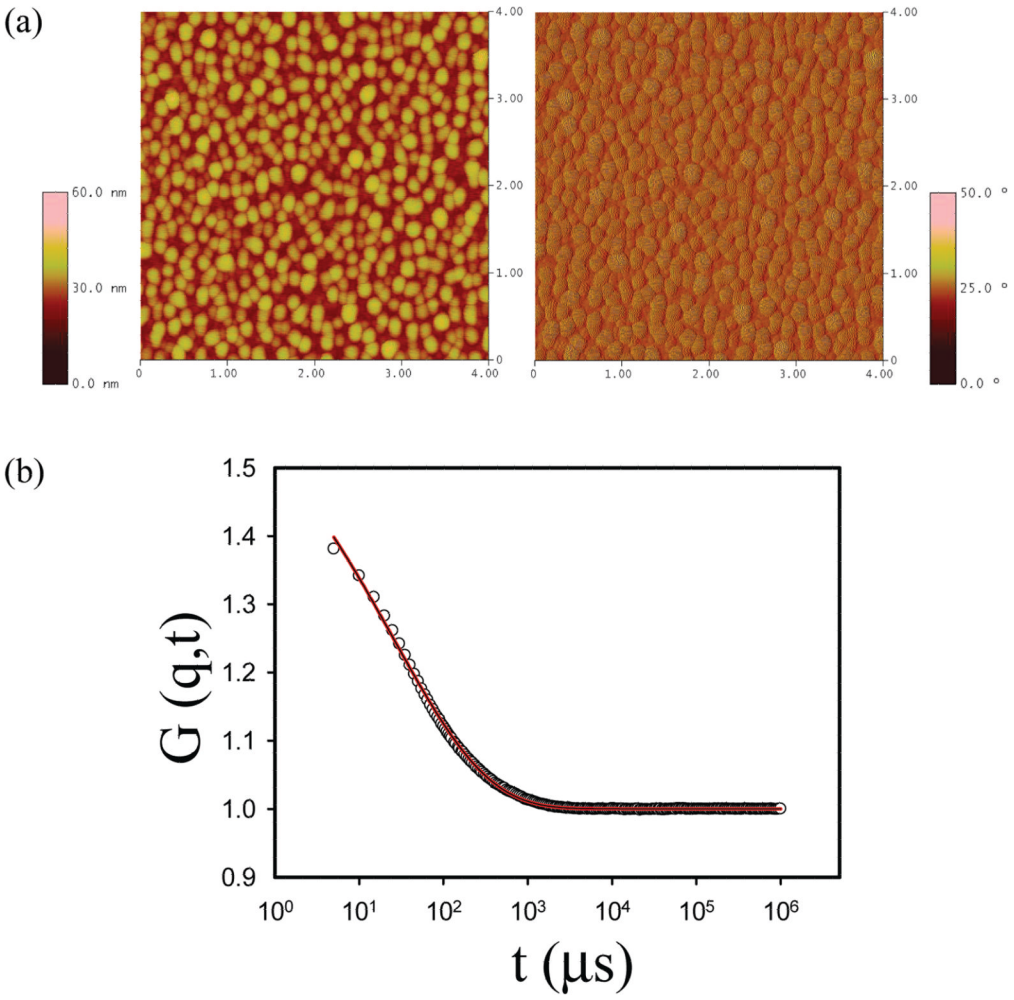

Figure 4.
(a) Surface morphology images of acylChitoMPEG. The left is height image and right is phase image. (b) Single stretched exponential fit for mean sizes of acylChitoMPEG nanoparticles.

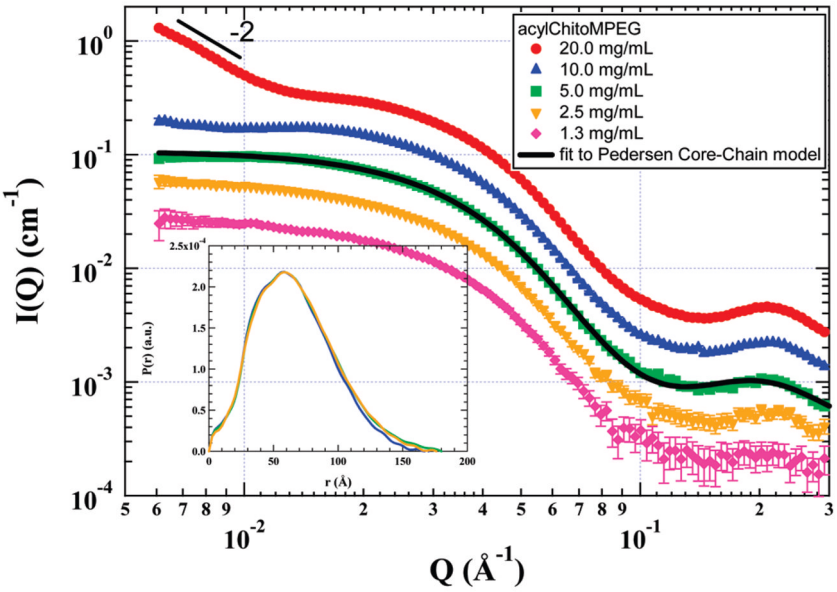

Figure 5.

The scattering profiles of the acylChitoMPEG solutions in water at different concentrations. The inset includes the pair-distribution functions calculated from the figure for acylChitoMPEG concentrations of 2.5, 5, and 10 mg/mL with data up to $Q = 0.5$ Å^{-1} using the program GNOM.[34]

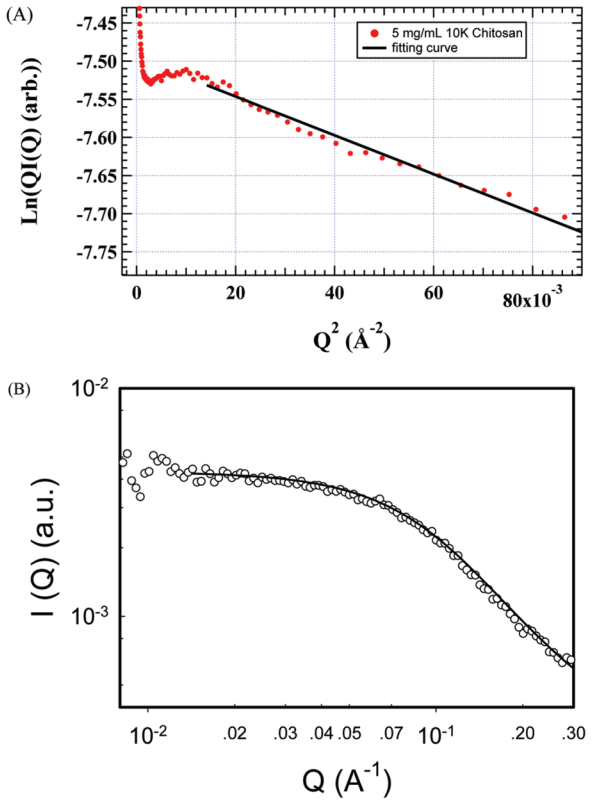

Figure 6.

(A) The modified Guinier plot of SAXS data of 5 mg/mL 10k chitosan in water. The solid line is the fit to rod-like polymers. (B) The scattering profile of 10 mg/mL 2k MPEG in water. The solid line is the fit to Debye function for flexible, Gaussian polymers.

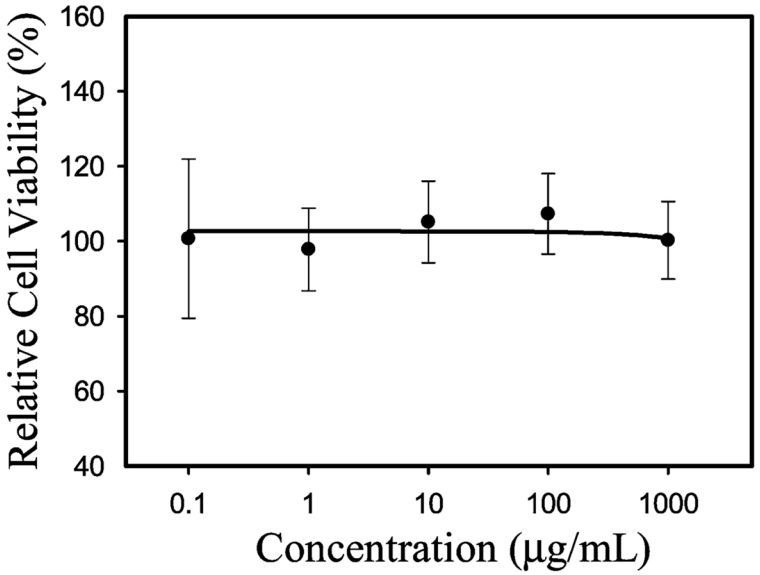

Figure 7.
Cytotoxicity of acylChitoMPEG in HepG2 cells. Mean ± standard deviation (*n* = 8).

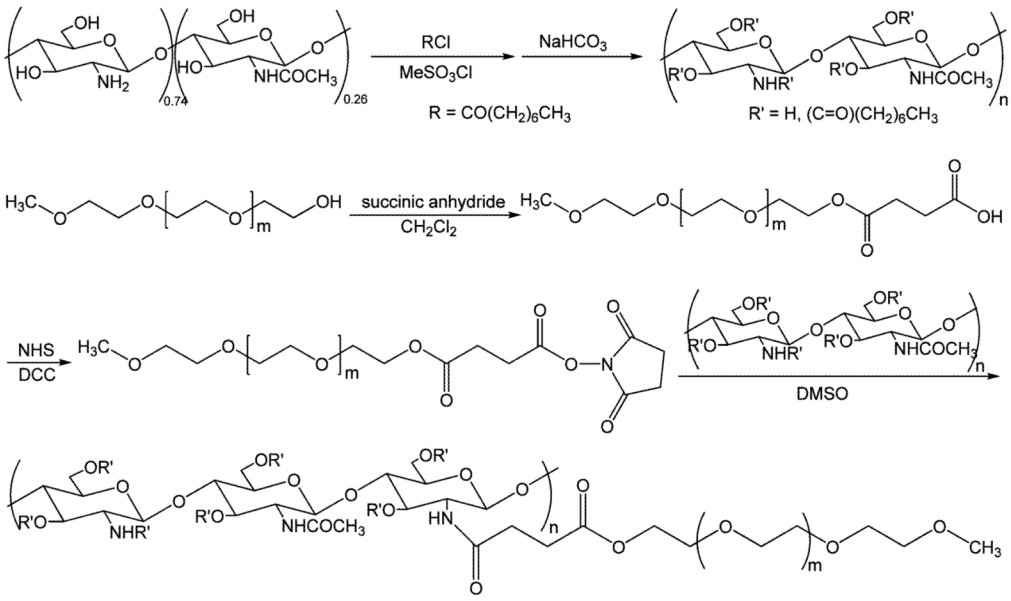

SCHEME 1.
Synthetic Scheme Used to Prepare AcylChitoMPEG

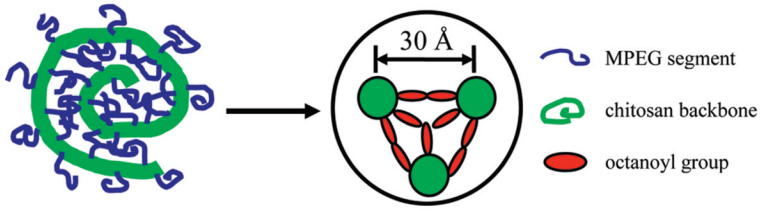

SCHEME 2.
The Coiled Structure of the Triple Helical AcylChitoMPEG Backbone

TABLE 1

Characterization of AcylChitosan

	DS[a]			
sample	**NH_2**	**NHAc**	**NHR**	**OR**
chitosan	0.74	0.26	0	0
acylChitosan	0.69	0.23	0.08	0.92

[a]The degree of substitution determined by ^{1}H NMR.

TABLE 2

Characterization of AcylChitoMPEG

sample	DS_R[a] = DS (NHR + OR)	DS_R/DS_M	DS_M[b]	Mn[c]
acylChitoMPEG	1.0	2.18	0.46	72.8k

[a] The degree of substitution of acyl groups.

[b] The degree of substitution of MPEG.

[c] The molecular weight determined by ^{1}H NMR.

TABLE 3

Solubility of Chitosan and Its Derivatives in Different Solvents[a,b]

sample	Milli-Q water	ethanol	acetone	CH_2Cl_2	$CHCl_3$	THF	dioxane
chitosan	+	−	−	−	−	−	−
acylChitosan	−	+	+	+	+	+	+
acylChitoMPEG	+	+	+	+	+	+	+

[a] The solubility tests were performed at room temperature, and the concentration was 5 mg/mL in each solvent used.

[b] Key: +, soluble; − insoluble.

TABLE 4

Self-Assembly Properties of AcylChitoMPEG

		diameter (nm)	
sample	**CAC[a] (mg/mL)**	**by AFM[b]**	**by SEF[c]**
acylChitoMPEG	0.066	17.6	24.4

[a] The critical aggregation concentration.

[b] The apparent particle diameter determined by microscopy.

[c] The mean particle hydrodynamic diameter determined by stretched exponential fit using dynamic light scattering.

TABLE 5

The Fitted Forward Scattering Value and the Calculated Association Number of AcylChitoMPEG at Different Concentrations by SAXS

***C* (mg/mL)**	**1.3**	**2.5**	**5**	**10**	**20**
I_0[a] (cm^{-1})	0.025 ± 0.001	0.055 ± 0.001	0.106 ± 0.001	0.209 ± 0.002	0.398 ± 0.002
n_{assoc}[b]	3.2 ± 0.1	3.5 ± 0.1	3.4 ± 0.1	3.3 ± 0.1	3.1 ± 0.1
R_g[c] (Å)	52 ± 2	54 ± 1	53 ± 1	51 ± 1	48 ± 1

[a]The scattering intensity.

[b]Association number.

[c]The radius of gyration.